A HIGH DYNAMIC RANGE REPLACEMENT CONCEPT FOR THE CANADA-FRANCE-HAWAII TELESCOPE

UH/IfA HDRT Study Committee:

J.R. Kuhn (Chair)
G. Moretto
R. Coulter
P. Baudoz
J. E. Graves
D. Jewitt
R. Joseph
R. Kudritzki
G. Luppino
R. McLaren
D. Mickey
M. Northcott
F. Roddier
C. Roddier
C. Shelton
A. Stockton
A. Tokunaga
J. Tonry
B. Tully
R. Wainscoat

CONTENTS

A High Dynamic Range Replacement Concept for the Canada-France-Hawaii Telescope

1 ABSTRACT

The High Dynamic Range Telescope (HDRT) expands on the 6.5 m aperture New Planetary Telescope which was devised as a replacement for the NASA Infrared Telescope Facility. The concept described here benefits from the ideas and from input from all three partner communities within the CFH consortium. As conceived, the HDRT will provide unprecedented photometric and angular resolution dynamic range. As the world's largest and highest resolution optical telescope it will also provide wide-field observations with an etendue significantly larger than even the special-purpose survey telescopes now in their planning stages. Beyond this, the HDRT allows unique opportunities for observing faint astronomical objects in the near environment of bright sources.

2 PRINCIPLES

Current optical technology now allows the possibility of building a telescope which maximizes the point-spread-function (PSF) core energy *while minimizing the scattered light flux in the wings of the PSF*. These are the key requirements for achieving high angular and photometric dynamic range that have contributed heavily to the HDRT concept.

It is clear that any CFHT replacement must use segmented or multiple mirrors to achieve an effective aperture of at least 15 m. How should mirror segments be arranged in the telescope pupil plane? Given that the cost per area for the primary mirror and its associated actuators is a significant fraction of the HDRT budget, we find that there are distinct advantages to a modestly "unfilled" pupil. The angular resolution provided by the larger unfilled aperture is an obvious potential advantage. The possibility of building a telescope with a pupil which is relatively open has additional optical and mechanical advantages which will become apparent below. We expect this new CFHT to incorporate a combination of technologies which involve elements of interferometry and conventional large telescope design.

How large should mirror segments be? Note that any modern design will use mirrors which are thin by existing CFHT standards. They are either so small that their actuators rigidly move the mirror segments, in the style of Keck, or larger but with actuators (having perhaps the same areal density as a small segment) which deform the subaperture mirrors (like all current 8 m telescopes).

Mirror segment edges are a fundamental concern. They are difficult to polish accurately. A mirror with a larger edge-to-area ratio diffracts correspondingly more energy to large angles. Straight-line edges in the pupil also tend to diffract light to larger angles than curved segments. We minimize the effects of wavefront errors due to mirror edges and large-angle diffraction by making the mirror segments as large as possible. Circular segments maximize this ratio and are the building blocks for the unfilled telescope pupil design of the HDRT.

The overall size of the "fictitious" HDRT parent optic is a critical telescope parameter, but in the range of 22-30 m we believe this telescope can use either conventional active "metrology" to rigidize the structure, or interferometric beam combining techniques. Our choice of 6.5 m off-axis segments is determined by polishing cost concerns (like the dimensions of the current REOSC optics tower), but their diameter also could vary, probably with predictible costs up to subapertures of 8 m.

The HDRT design leads to an open structure which retains many of the technical advantages of a single 6.5 m off-axis telescope [1-3]. The particular parameter choices used here yield a total collecting area significantly larger than a "conventional" 15 m telescope with a mechanical support structure that encourages a large range of optical configurations. Our choice of a parabolic primary is driven by several technical advantages. These include the existence of a real prime focus, the possibility of highly efficient coronagraphic observing, and the natural ability to also achieve wide-field performance using two additional optics.

The HDRT achieves the effective light collecting area of an unobstructed 15.9m diameter telescope by using six 6.5 m off-axis mirror segments. This optical configuration will allow three distinct optical operating modes from the same facility: 1) a full AO compensated F/15 coronagraphic telescope with a diffraction limited field-of-view (FOV) of at least 10 arcsec and resolution of 12 milliarcsec at one micron (with the expectation of reduced AO performance over larger fields), 2) a moderate (but designated "narrow" field) F/15 mode optimized across a 3x3 arcmin^2 FOV, and 3) a wide-field F/1.3 mode (optimized across a 1x1 deg^2 FOV). The parent optic of the 6x6.5 m off-axis mirrors is determined by the likely physical envelope of the CFH enclosure – greater off-axis distances could be accommodated in larger (i.e. 30 m) designs.

A complete cost study has not been undertaken, but REOSC (Paris-France) has expressed their ability and willingness to build these optics. The critical issues for the M1 fabrication are the parent optical speed, diameter, substrate thickness, and surface smoothness requirements. We believe the optical elements described here, using a 6x6.5 m primary generated from a 22 m F/1 parabolic parent, are within the capabilities of more than one large optics fabrication facility.

2.1 Segmented or Distributed Mirrors?

We consider two alternatives for achieving a 15m-class CFHT replacement. Figure 1 shows pupil functions for a Keck-style (KS) segmented design and the HDRT. The hexagonal design assumes a mirror segment comparable to Keck's but it requires one more "ring" of elements (5) with the first and second rings obscured by the secondary (also scaled from the Keck design). This implies a total of 54 mirror segments. The HDRT design uses six 6.5 m unobstructed circular mirror segments from a 22 m diameter parent.

The Keck-style hexagons simulated here are separed from nearby segments by about 2% of a segment "diameter" (twice the side length). The actual edge separation of Keck telescope segments is smaller, although it is likely that the wavefront distortion due to mirror edge polishing errors will have a *larger* effect than we account for with this approximation. Figure 2 gives an indication of the actual wavefront errors for the Keck mirrors. This was obtained from the differ-

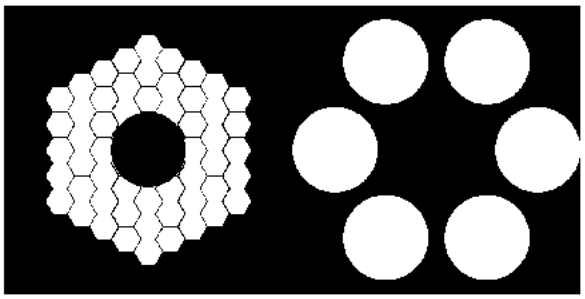

Figure 1: *Pupil functions for Keck-style (left panel) and HDRT (right panel) primary mirrors. Each panel corresponds to an area 22 m on a side.*

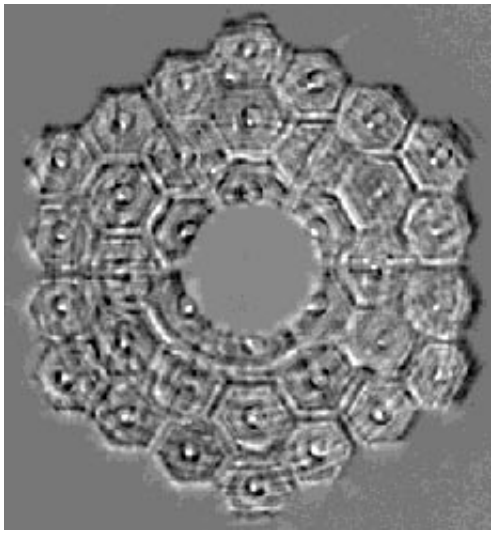

Figure 2: *Wavefront errors measured from out-of-focus images obtained at the Keck telescope [4]. The full range between black and white corresponds to a phase error of about one wave in the visible.*

ence of out-of-focus images obtained with LRIS. The image greyscale here indicates the local wavefront curvature over a spacial scale of a few centimeters. Mirror edges are easily visible at most segment boundaries with errors that can be as large as one wave. The primary effect of these wavefront errors is to increase the scattered light out of the image core. The mirror boundary errors also tend to limit the high spatial frequency correction achievable with an adaptive optic system and to increase the temporal bandwidth needed for the same degree of wavefront correction. We will illustrate this with calculations based on the pupil functions from Fig. 1.

Table 1: *Core Energy Concentration and Angular Resolution*

Pupil	AO (d.f.)	Peak	FWHM ["]	E_0
HDRT	400	0.050	0.017	0.149
KS	400	0.032	0.025	0.116
HDRT	0	2.7e-4	0.33	6.3e-4
KS	0	2.8e-4	0.33	3.3e-4

To account for the effects of the atmosphere we've added a Kolmogorov phase screen with an outer scale of about 22 m and Fried length of 1m. We also assume a wavelength of 1 μm. To estimate the effects of adaptive optics (AO) we model this system as if it estimates the atmospheric phase errors using an interpolating function with a specified number of degrees of freedom. In the calculations here we consider an AO system with 400 degrees of freedom across the non-zero domain of the pupil. Table 1 illustrates how the core image peak height (proportional to the delivered Strehl) and the full-width at half-height of the image core (derived from a Gaussian fit) and the energy within the first Airy ring (E_0) are affected by AO and the pupil configuration (Keck-style–'KS' versus 'HDRT'). While there is very little difference in the imaging capabilities of these telescopes at 1 μm without adaptive optics, there clearly is a realizable difference using a "modest" AO system – one using subapertures which are no more complex than the current curvature system now being implemented by the IfA/UH for the Gemini 8m telescope. The HDRT achieves at least 65% improvement

in the core energy in point source observations with nearly a 50% improvement in the effective angular resolution.

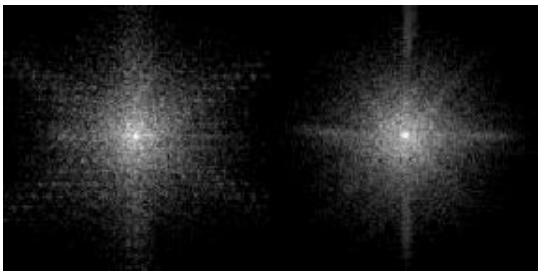

Figure 3: *Keck-style (left) and HDRT (right) point source images using a 400 degree-of-freedom AO system. The intensity scale is logarithmic and the angular size of each panel is 4.6 arcsec.*

Figure 3 shows point source images resulting from the 400 d.f. AO system on the Keck-style and the HDRT pupils. Both panels were plotted with the same logarithmic intensity scale and the angular size of each image is 4.6 arcseconds.

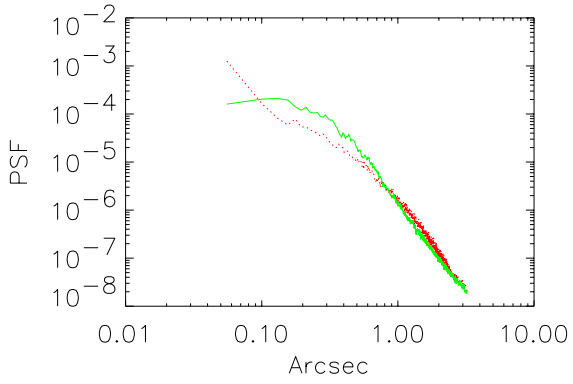

Figure 4: *HDRT PSF with AO (dotted line/red) and without AO (solid line/green) are plotted here.*

Figure 4 shows how the circular average PSF of the HDRT is affected by a 400 d.f. AO system. Here the dotted line shows the PSF without AO. As expected, the AO system achieves significant correction out to about 0.3 arcsec with essentially no effect on the PSF at larger angles. The PSF from the segmented mirror using AO shows several important differences. Figure 5 compares the AO-corrected segmented and HDRT PSFs. The most obvious difference is that the segmented mirror has more scattered light at angles larger than 0.3 arcsec. Even though these curves are generated from the circularly-averaged light profiles, the first diffraction peak at 0.2 arcsec appears prominently in the segmented mirror telescope.

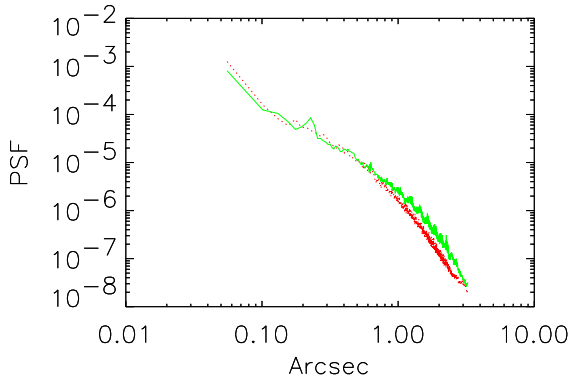

Figure 5: *Keck-style (solid line/green) and HDRT (dotted line/red) AO corrected PSFs are displayed here.*

Without adaptive optics the performance of the two telescope configurations is comparable. With a simple, first-light, AO system these calculations show that there is a significant penalty in Strehl ratio and scattered light for a hexagonal segmented mirror in comparison to the HDRT.

3 OPTICS

The open HDRT pupil configuration also implies important optical and mechanical advantages. We illustrate these points with

more detailed geometrical descriptions of the optics needed to achieve wide- and narrow-field operation.

3.1 Narrow-Field Mode

The telescope narrow-field mode (NFM) uses a two-mirror Gregorian optical configuration. The parent is a 22 m F/1 parabola from which we use an array of 6x6.5 m off-axis sections. The optical path beyond the prime focus will be completely accessible along a structural optical bench that is parallel to the parent optical axis of the telescope, and is outside of the optical path of the decentered light path from each 6.5 m off-axis primary mirror segment.

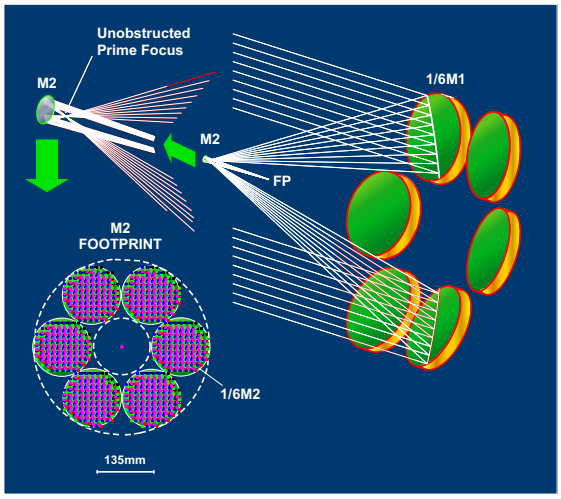

Figure 6: *The HDRT concept uses six sub-apertures for the Narrow-field Mode.*

The NFM illustrated in Figure 6 was optimized to produce an F/15 system across an isoplanatic 3x3 arcmin FOV, with an effective focal length (EFL) of 330m and a plate scale of S=0.625 arcsec/mm. Very small M2 mirror segments are possible. In this way any instrument that requires a FOV smaller than a few minutes of arc can use a secondary telescope mirror comparable to the size of its internal optics! Since the light path is fully accessible beyond M2 without obstructing M1, astronomical instruments may be designed to include their own specialized secondary telescope mirror or mirror segments. For example, instruments mounted near the top of the HDRT are well suited for implementing cryogenic or adaptive secondary optics as subcomponents of the NFM instruments.

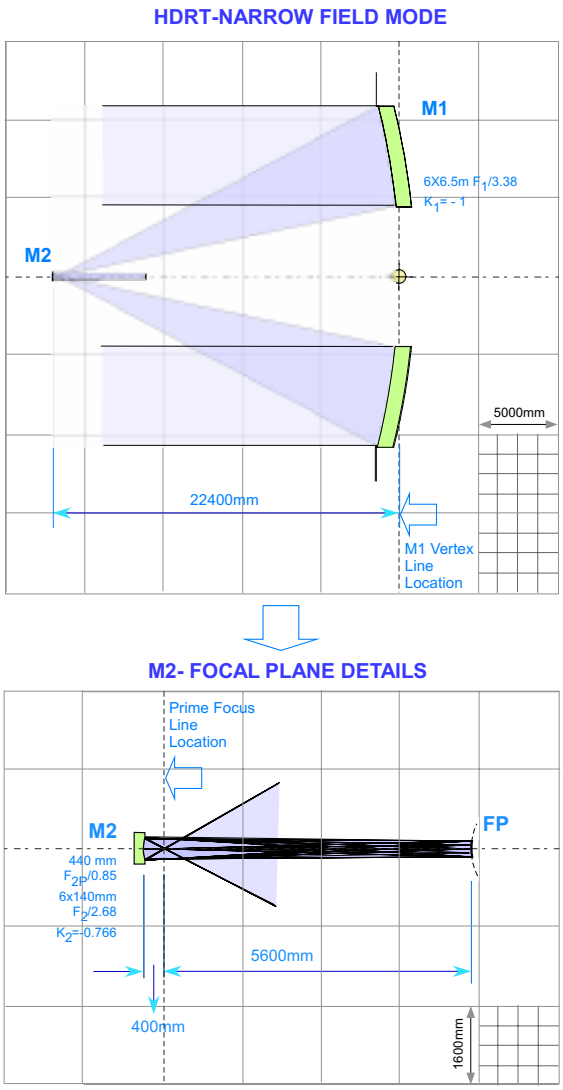

Figure 7: *The HDRT narrow-field mode (NFM-6) concept. M2 can be as small as 0.4m in diameter or composed of six 140mm optics.*

One NFM-M2 mirror is possible, but for tip-tilt and alignment purposes it may

Table 2: *HDRT Narrow Field Configurations*

Design	M2-PF (m)	Blur (arcsec)	M2 dia. (mm)
NFM-6	0.4	0.120	420
NFM-8	0.53	0.100	553
NFM-10	0.66	0.083	685
NFM-12	0.80	0.072	820
NFM-14	0.93	0.071	952
NFM-18	1.20	0.062	1220

Table 3: *Optical Prescription for HDRT NFM-6. The effective focal length is 330 m yielding a focal ratio of F/15 and plate scale of 0.625 arcsec/mm*

Surf.	Rad.[mm] (Conic)	Thick.[mm]	Aperture (Parent)
M1	-44000	-22400	6x6.5 m F/3.38
	(-1.0)		(22 m F/1)
M2	749.8	6000.	6x140 mm F/2.68
	(-0.77)		(0.42 m F/0.85)
FP	457.9	–	288 mm x 288 mm
	(0)		

be useful to use six separate off-axis mirrors for the secondary optics. In this case each M2 subaperture illumination pattern must not touch. This yields a constraint on the FOV and the distance of the parent M2 vertex from the prime focus (PF), here designated M2-PF. Several optimizations (Table 2) were done as a function of the distance between the M2 vertex and the focal plane, M2-FP. In the table the "blur" is computed from the 80% encircled energy diameter. The shortest possible design was obtained with M2-FP of 6 m which we designate NFM-6 below. Its optical prescription is presented in Table 3 and the layout of NFM-6 is shown in Fig. 7. The distance between the prime focus and gregorian focal plane (FP) here is 5600 mm with an effective focal distance of -330 m and a system focal ratio of F/15.

This is not a natural Gregorian design for the NFM as it was optimized with the constraint of a small M2 and short PF-FP distance. Other optimizations were done for longer designs – M2-FP varying from 8.0 m to 18 m, which require a larger secondary mirror, as described above, but which yield better performance than the shorter NFM-6 design. In all NFM optimizations (NFM-6 to NFM-18) the M2 mirror is a concave oblate ellipsoid with small variations of the conic constant (less than one percent). The Gregorian focal surface is concave down with a radius of curvature of about 0.5 m. This can be corrected within the instruments as is often done in conventional telescopes.

If HDRT uses a shorter NFM design the geometric spot blur will be degraded, but even the shortest design (NFM-6) with the "worst" performance achieves a blur diameter of 0.091 arcsec FWHM at the edges of a 3x3 arcmin^2 FOV. Figure 8 shows the NFM geometrical spot performance across a 3 arcmin FOV. The design space for the HDRT NFM allows several mechanical options to be explored. The best design will be determined by considering the mechanical constraints imposed by a versatile optical configuration which allows both wide- and narrow-field performance with minimal

configuration change overhead.

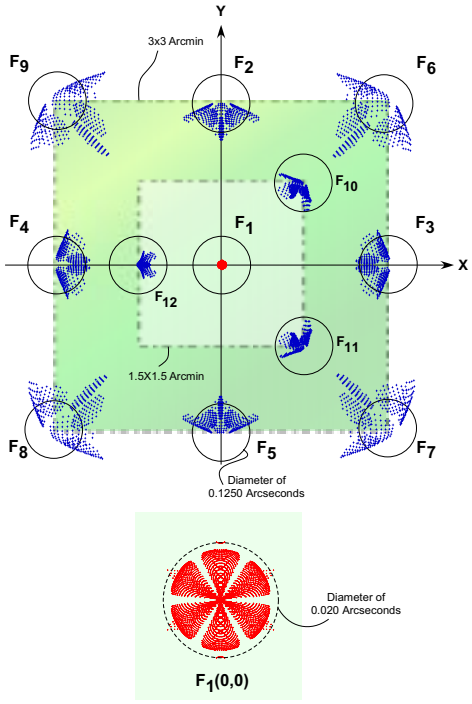

Figure 8: *NFM-6 geometrical spot diagrams computed across a 3x3 arcmin^2 FOV. The reference circles are 0.130 arcsec and 0.020 arcsec is used for the center field.*

Over a small field-of-view, suitable for AO and coronagraphy, the HDRT must be diffraction-limited. This is achieved even with the most compact NFM-6 design. Figure 9 shows that this design on a 10 x 10 arcsec^2 FOV is diffraction limited to wavelengths as short as the R band (700 nm). Figure 9 shows the optical performance of NFM-6 over the full 3 arcmin FOV. Achieving this resolution will depend on implementing active and adaptive optics control in the baseline HDRT telescope design.

3.2 Wide-Field Mode

To provide the HDRT with a wide-field (WFM) imaging and spectroscopic mode we consider an F/1.9, system optimized over a 1x1 deg^2 FOV. A field-of-view of 2x2

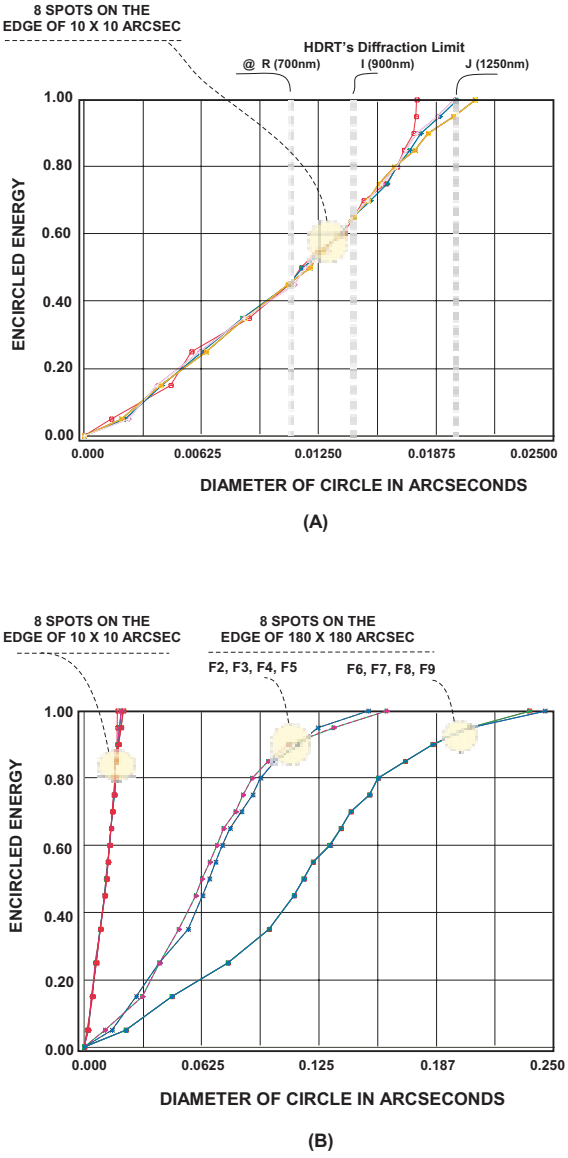

Figure 9: *The HDRT NFM encircled energy performance:* **(A)** *This panel illustrates the radial distribution of the enclosed energy and the diffraction limited performance of the system in a 10x10 arcsec^2 field. The dashed-gray-lines indicate the diffraction limits for HDRT at 700, 900 and 1250 nm.* **(B)** *The overall performance of the system for each field position $F_n(x, y)$, as defined in figure 8, across the 3x3 arcmin^2 FOV.*

deg^2 is also possible with slightly larger spot sizes and a larger M3. Using the NFM 6x6.5m off-axis primary mirror described above we obtain an off-axis Paul-Baker configuration by adding convex secondary (M2-WFM) and concave tertiary (M3-WFM) corrector mirrors. A conventional Paul-Baker configuration, produces excellent correction across a wide FOV but typically also suffers from significant obscuration because of the large secondary and tertiary mirrors (*cf.* Moretto and Kuhn 2000 [2]). For the HDRT concept this obscuration is only a few percent because the primary uses decentered mirrors. In this case the secondary (M2-WFM) and tertiary (M3-WFM) mirrors can be placed outside of the optical path of each 6.5m primary mirror segment.

The requirement for fast optics here is driven by the need to develop an affordable (0.5 m diameter) focal plane. We have achieved a plate scale of 4.93 arcsec/mm with a system focal ratio of F/1.9. Other WFM configuration constraints have also been considered: (1) a shorter telescope design using a shorter distance between the M1 vertex and M2-WFM, and (2) a shorter corrector design, that uses a smaller distance between M2-WFM and M3-WFM vertices, (3) smaller diameter mirrors for M2-WFM and M3-WFM.

The natural WFM design is a longer configuration with an M2-M3 distance of 24m (WFM-24). In this case the tertiary mirror (M3-WFM) is located 8.9 m behind the primary mirror M1 vertex, and the M2-WFM vertex is 15.5 m from the M1 vertex, as shown in Figure 10. The M2-WFM diameter is 7 m, but only six off-axis sections of the secondary mirror (M2-NFM) are illuminated. Thus M2-WFM is built from an array of six small off-axis mirrors each 2.3 m in diameter. The M3-WFM diameter is 7 m and is a single mirror. Table 4 displays the optical prescription for WFM-24.

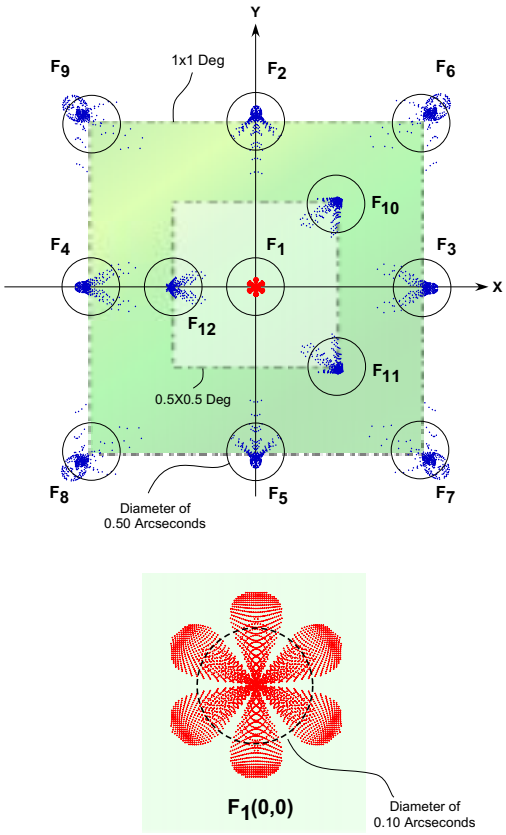

Figure 11: *The HDRT-WFM geometrical spot performance. Spot diagrams are computed across the 1x1 deg^2 field.*

The resulting geometrical spot performance across this large field is excellent. Figure 11 shows the HDRT-WFM spots with a detail of the central spot pattern. Figure 12 plots the encircled energy.

Several designs were optimized as a function of the M2-M3 distance while keeping M1-M2 close to 18-19 m. A comparison is shown in Figure 13 in terms of the blur diameter optical performance for each geometry. Each point shows the mean value of the blur circle diameter with 80% and 50% ($\sim$ FWHM) of encircled energy for the 8 spot positions at the edge of the flat 1x1 deg^2 FOV. The long-design (WFM-24) performance is represented by the two points at the bottom right side of the Fig. 13. The

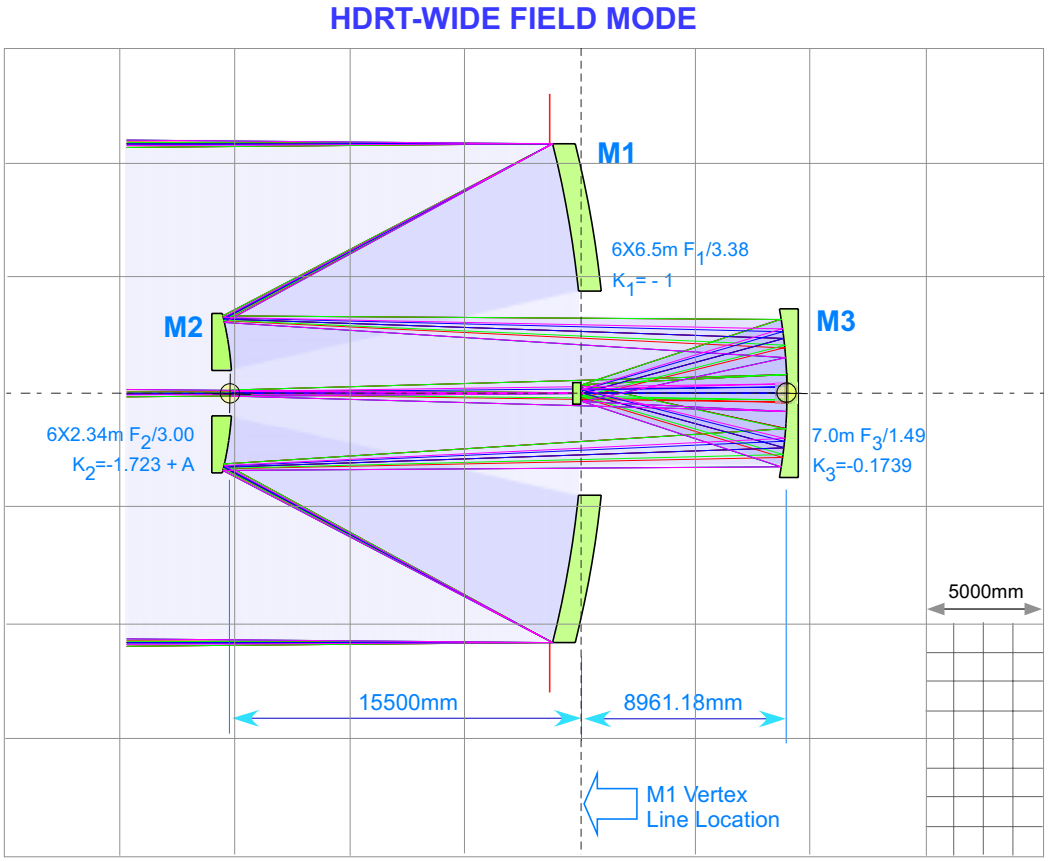

Figure 10: *HDRT-WFM layout, the effective focal length is EFL=-41838 mm resulting in a F/1.90 focal ratio and a plate scale of 4.93 arcsec/mm. The position of the tertiary mirror M3 and focal plane FP were constrained during these optimizations.*

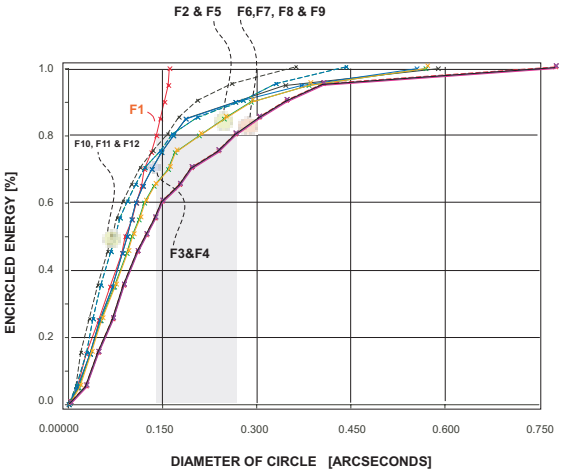

Figure 12: *The HDRT-WFM encircled energy distribution for each field position $F_n(x, y)$, as defined in figure 11, across the 1x1 deg^2 FOV. The shaded region represents the range of EE diameters, in arcsec, where the spots contain 80% of the energy.*

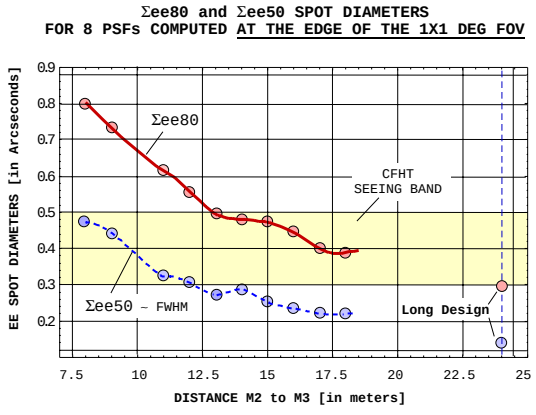

Figure 13: *Variation in WFM optical performance versus M2-M3 distance.*

distance M1-M2 is not constant as M2-M3 varies, but ranges between 18m and 19.4m. The figure shows that designs with M2-M3 larger than about 12m achieve seeing-limited optical performance across the full 1 degree FOV. A solution for a 2x2 deg^2 field will require M2 mirror segments that are 2.6 m in diameter and an M3 which is 8.1 m. The mean rms and 80% energy spot diameters across the field in this design are 0.30 and 0.53 arcsec.

3.3 Mounting WFM and NFM

This open pupil structure allows access to the HDRT optical path along an "optical bench" that extend up through the core of the telescope. This makes it feasible to design a telescope which can change from NFM to WFM without perturbing the instruments or optics. Thus we envision a telescope facility which has NFM and WFM instruments permanently mounted, along with all secondary optics, on a central core of the optics support structure (OSS) truss. As we show below, it is possible to design an OSS that accommodates WFM and NFM optics by folding the 6 WFM M2 mirror segments up or down like petals on a flower. This mechanical structure will be actively "stiff" and should simultaneously support all optics and NFM instruments.

The solution we favor combines the WFM-24 and NFM-6 configurations as is shown in Figure 14. The focal plane for the NFM is 40mm above the vertex of the M2-WFM. More accurately, FP-NFM is inside of the M2-WFM's 2 m central aperture (see also Fig. 15). This allows room for the NFM instruments and AO systems if light is also folded out into the clear volume beyond the NFM-M1 optical path to M2 (but see below). To increase the instrument volume

we can also move M2-WFM closer to the M1 vertex. In this way there is less chance for interference between M2-WFM and FP-NFM. In this modified WFM-24 design the distance between the M1-vertex and M2-WFM vertex is 15.5 m, instead of 16.4 m for the WFM-24 design. This results in a separation between the M2-WFM vertex and FP-NFM of 900mm. There is no optical performance penalty - just the diameter of M3-WFM increases from 6.10m to 6.74 m and the M2-WFM mirror segments grow from 2.1 m to 2.3 m. The WFM focal plane is near the vertex of the M1 parent and there is ample access from the back of M1 for imaging and spectroscopic instrumentation. Although the WFM focal plane is obscured, depending on the size of the WFM instrumentation, this obscuration will be only a few percent.

3.4 Optical Fabrication

The optical requirements of the HDRT are non-trivial, but well defined and with a clear path toward a comfortable optical fabrication process. We have had two meetings with REOSC to verify the feasibility and likely budget requirements for the large off-axis mirrors and the aspherics. At our second meeting at REOSC in October 2000 a baseline optical test (a modified Maksutov) was outlined for the off-axis parabolic M1 segments – our most pressing optical manufacturing issue. Figure 16 describes the primary mirror surfaces in the baseline design.

The baseline NFM secondary mirrors are small and are not a significant technical concern. Their cross-section and relative geometry are indicated in Figure 17.

The optical prescription for the WFM secondary and tertiary are described in Table 4. Figure 18 illustrates the WFM M2

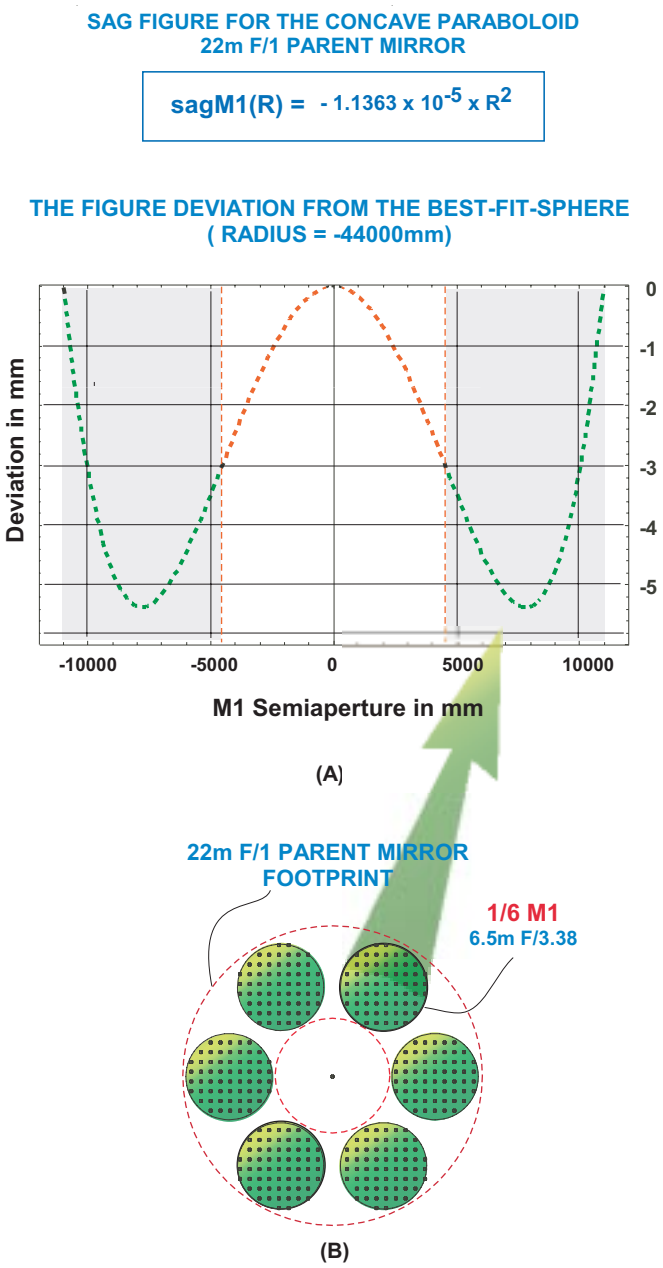

Figure 16: *The HDRT primary mirror M1 surface.* **(A)** *shows the deviation from the best-fit-sphere for the parent primary mirror, a pure paraboloid. The shaded region indicates the radial extent of each subaperture of the parent mirror.* **(B)** *shows the geometry of each of the subapertures. Each of the six 6.5 m diameter subapertures define an F/3.38 beam which intersects at the telescope prime focus 0.4 m below the secondary mirror vertex.*

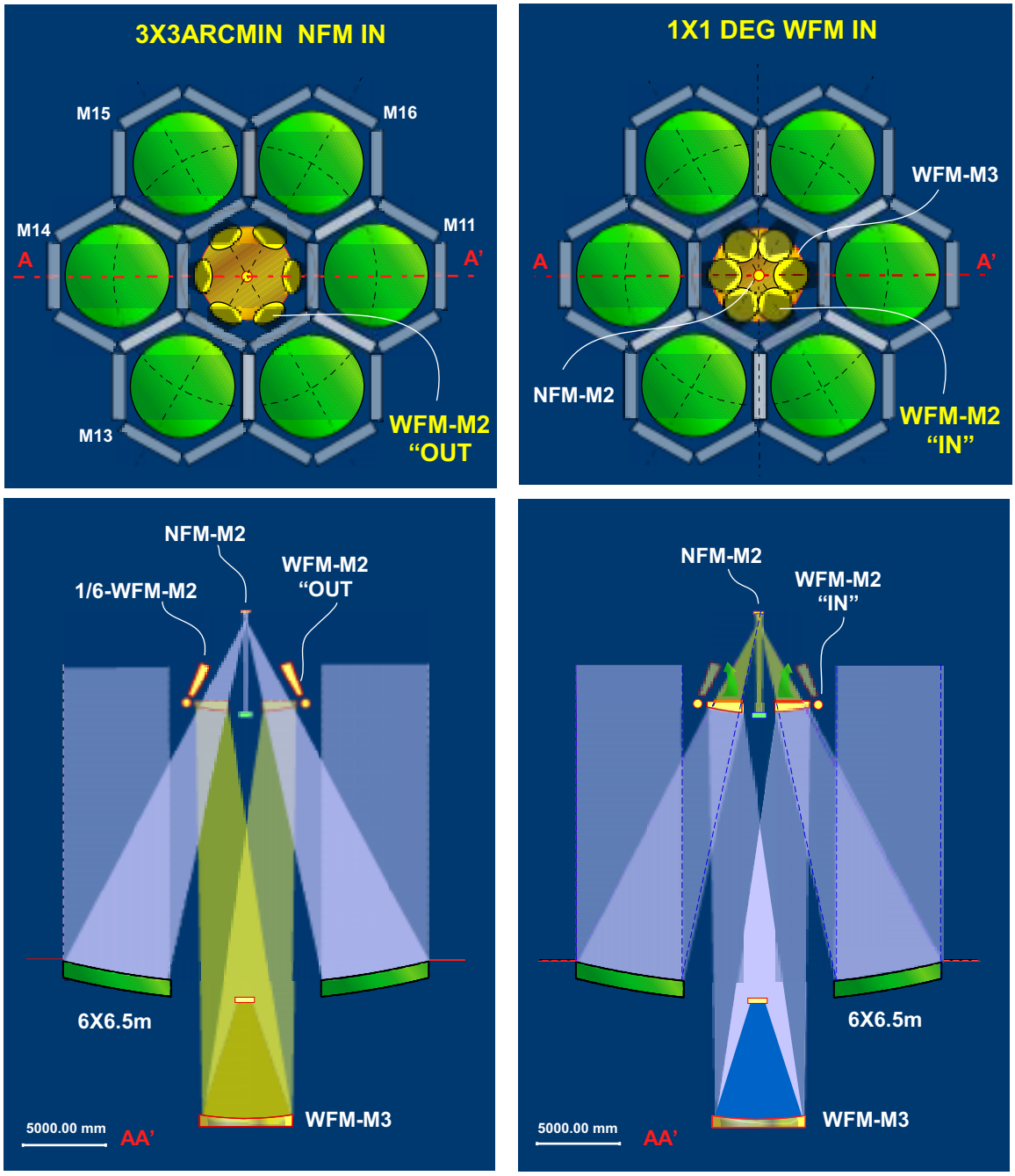

Figure 14: *The permanently mounted HDRT design combining WFM + NFM. The distance from the vertex of WFM-M3 to WFM-M2 is 24.461 m and the vertex distance from NFM-M2 to its FP is 6 m. The distance from M1 vertex to WFM-M2 is 15.5 m and the M1 vertex to NFM-M2 is 22.4 m. The NFM design produces a subaperture-M2 mirrors of 140mm diameter. The diameter for WFM-M3 is 7.0 m and the subaperture mirrors are 2.34 m.*

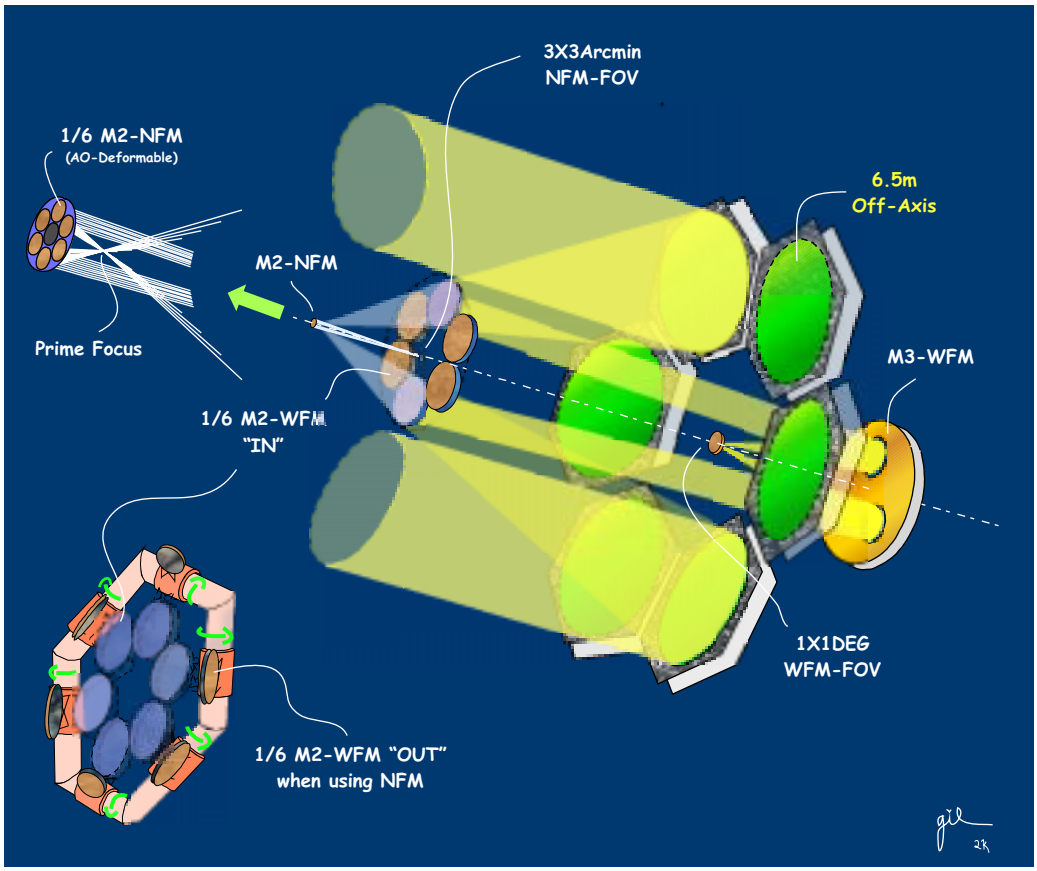

Figure 15: *The full HDRT optical layout is shown here. At the bottom-left corner of the figure, M2-WFM is composed of six subaperture mirrors and they can be separately folded up or down - like petals on a flower - out of the way of the NFM light path. At the top-left of the figure we see the six narrow-field subaperture mirrors that are 140mm in diameter, and the unobstructed prime focus.*

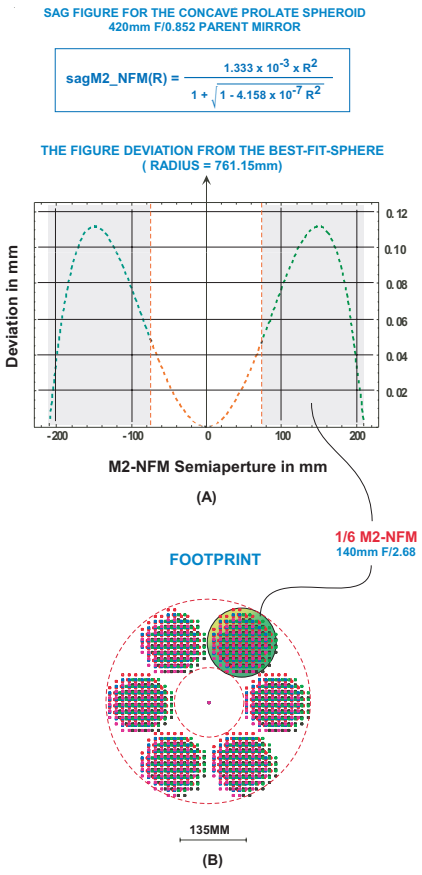

Figure 17: *The HDRT-NFM secondary mirror M2 surface.* **(A)** *shows the deviation from the best-fit-sphere for the parent secondary mirror, a pure conic ellipsoid with its major axis on the optical axis. The shaded region indicates the radial extent of each subaperture of the parent mirror.* **(B)** *shows the geometry of each of the subapertures. Each of the six 140 mm subapertures define an F/2.68 optical beam that interects at the gregorian focus about 6 m below M2.*

mirror profile. M2 is a hyperboloid (k=-1.7234) plus a 4th order polynomial deformation. This figure also shows the isolated illumination pattern on the mirror. These optics have a significant aspherical departure but it is not unreasonable to achieve this figure with six 2.3 m F/3 mirrors.

Figure 19 shows the M3 mirror geometry. M3 is a pure conic ellipsoid (k=-0.1739) and its aspheric departure is modest, although it is large (about 7 m). It is fully illuminated and cannot be sectioned.

4 TELESCOPE MECHANICAL STRUCTURE AND ENCLOSURE

We have only begun to look at very simple trial telescope structures which could accommodate the HDRT optics and instruments. While there are many desirable features to an equatorial mount we are reluctant to propose this as a baseline for HDRT because of the complexity and size this adds to the enclosure. Our baseline OSS configuration would be an altitude-azimuth telescope. One example is shown in Figure 20 below. The use of active alignment elements for some of the trusses in this OSS may allow a total moving mass of 350 T or less, but considerable work remains to be done to define a more realistic mechanical HDRT mount. Discussions with a major engineering firm have been initiated to improve this concept [5].

The enclosure for a 22 m telescope is a significant engineering feat. While we have not had resources to pursue a careful trade study we believe that a leading candidate will be a comoving structure in the style of the Sloan telescope. Such a building could

Table 4: *Optical Prescription for HDRT-WFM. The system effective focal length is EFL=-41838 mm, giving a system focal ratio of F/1.90 and plate scale of S=4.93 arcsec/mm.*

Surface (M_n)	**Radius** mm	**Thickness** mm	**Shape** (K_n)	**Aperture** (Parent)
M1	-44000.0	-15500.00	-1.00	6 × 6.50m – F_1/3.38 (22m – F_{1P}/1)
M2	-14011.4	24461.2	-1.72 + A	6 × 2.34m – F_2/3.00 (7m – F_{2P}/1)
M3	-20872.2	-9003.2	-0.17	7.0m – F_3/1.49 –
FP	Flat	–	–	730.22mm × 730.22mm

readily be built with angled reflective panels which minimize the visual impact from every location on the Big Island. Such a structure could also be accommodated within the 40 m height limit for the CFHT site. Figure 21 shows how one concept might look. In this image the two building halves separate to expose the telescope and then rotate with the telescope azimuth.

5 SCIENCE PRIORITIES

The HDRT is not a specialized telescope. In fact the technology it uses will make it the largest and most versatile facility for optical and infrared astronomy for many years. The likely scientific targets of such a large aperture telescope (with even better spatial resolution in the case of HDRT) have been described for every next generation telescope now under consideration. We will not repeat the chorus here. The principal advantage of the HDRT over other concepts is its dual impact on both narrow-field and wide-field astrophysical targets. Since the HDRT is fundamentally a primary mirror plus an optical bench, we believe it also offers the greatest potential for future scientific impact – beyond what we might even now conceive. We illustrate a unique example of the HDRT's performance for narrow-field science, and summarize its likely wide-field scientific impact.

5.1 Example: Narrow-Field Observations

One of the most exciting capabilities of the HDRT will be its capacity for observing fields near bright objects. Figure 3 already gives an indication of how HDRT will outperform segmented-mirror telescopes. The reduction of scattered light at angles of a few tenths of an arcsecond is critically important, for example, in the optical search for faint stellar companions. We can illustrate this by modelling the performance of HDRT with a Lyot coronagraph. For

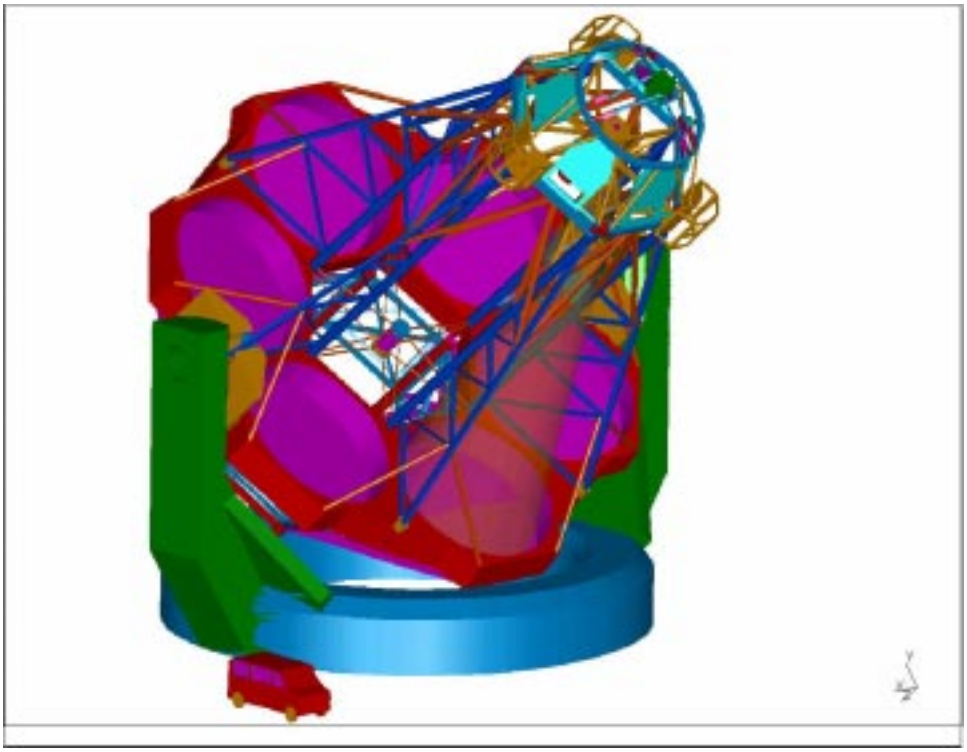

Figure 20: *HDRT optical support structure concept.*

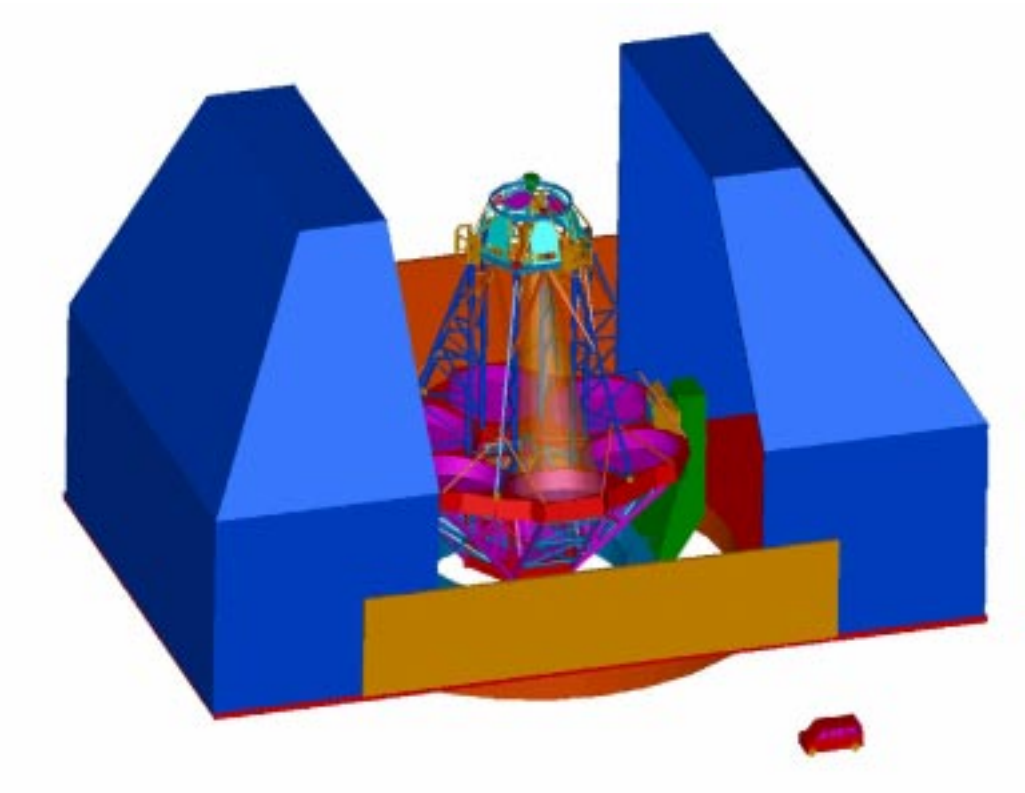

Figure 21: *HDRT enclosure concept.*

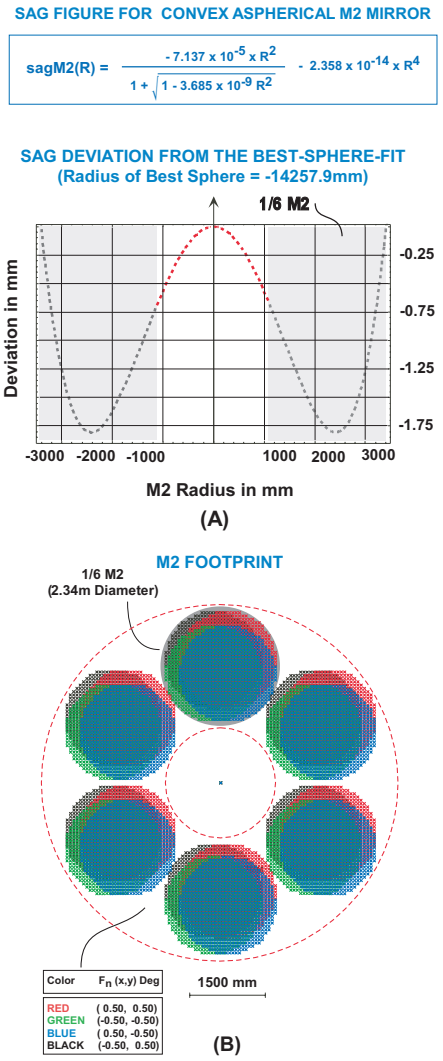

Figure 18: *The HDRT-WFM secondary mirror M2 surface.* **(A)** *Shows the sag shape and aspheric departure.* **(B)** *shows the illumination pattern on M2 from the primary. M2 naturally divides into 6 2.34 m mirrors.*

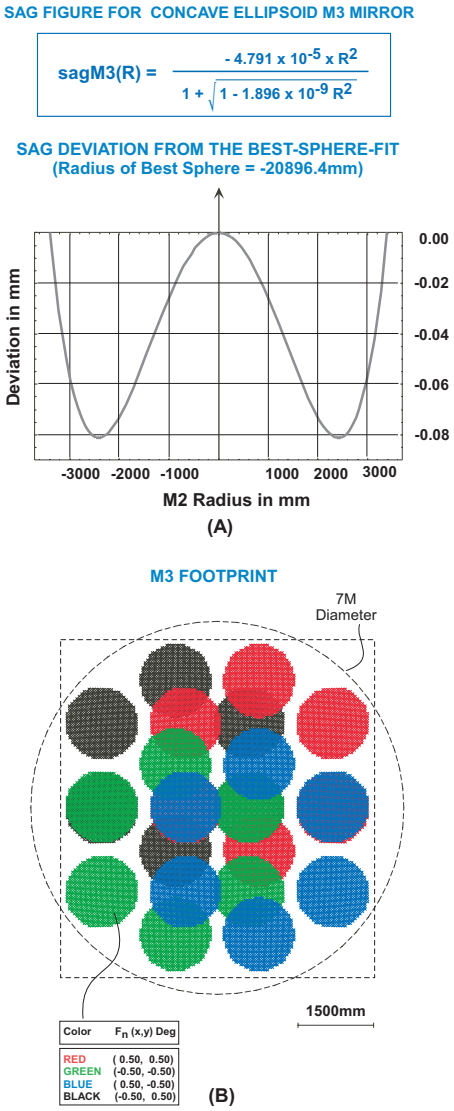

Figure 19: *The HDRT-WFM tertiary mirror M3 surface:* **(A)** *Shows the sag shape, and aspheric departure.* **(B)** *describes the illumination pattern on the mirror*

this we assume an AO-corrected wavefront (R_0=1m) with 400 degrees of freedom at a wavelength of 1μm using an image-plane occulter with a radius of 0.091 arcsec (ten pixels in our computational domain). Figure 22 shows what the pupil image immediately before the Lyot stop would look like. The effect of the occulter is to "high-pass"-filter pupil-plane spatial frequencies. Thus the pupil looks like a "phase contrast" image of the atmospheric wavefront errors which are particularly amplified near all pupil edges.

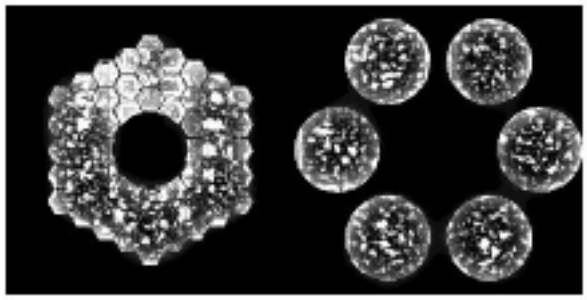

Figure 22: *Pupil images of the Keck-style (left) and HDRT (right) telescopes are shown here reimaged after a 0.091 arcsec occulter.*

The coronagraph reduces scattered light by re-imaging the object through a Lyot mask which blocks some of the diffracted light from the pupil edges. We occult the edges by generating a pupil mask which decreases the linear radii of the hexagonal segments or the circular mirror segments by 20%. The resulting PSFs for the two telescope coronagraphs are plotted in Figure 23. Beyond a few tenths of an arcsecond the coronagraphic performance of the HDRT surpasses the KS configuration by over half an order of magnitude.

The problem of photometrically detecting faint companions is fundamentally limited by systematic sources of scattered light. Figure 24 shows images obtained from an average of 64 seeing realizations using our 400-actuator AO system on the KS and HDRT telescopes. Each image shows a square 1.1 arcsec region and the data have been normalized to a constant central peak intensity. A faint companion that is 1% of the central source is 0.36 arcsec from the center. The detection problem for the KS telescope is obvious – false speckle and diffraction peaks prevent the identification of the companion. On an alt-azimuth telescope the speckle and diffraction pattern will also rotate with respect to the sky at rate that depends on the telescope altitude and azimuth.

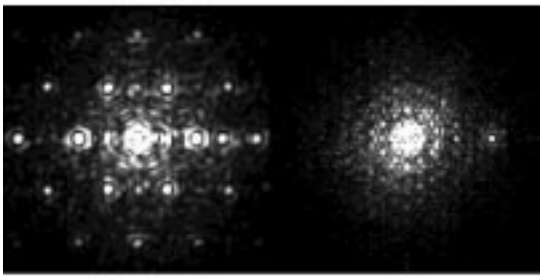

Figure 24: *Seeing averaged images (displayed on a linear intensity scale) from KS (left) and HDRT (right) telescopes. A faint companion is 0.36 arcsec to the right of the central star in each image.*

A coronagraph helps the detection problem in both telescopes, but it does more to improve the faint object capabilities of the HDRT. Figure 25 shows a seeing averaged image obtained with a coronagraph on each telescope. These data are displayed on the same linear scale as fig. 24. We estimate that the companion detection threshold for the HDRT will be between 1 and 3 magnitudes fainter than the KS under comparable conditions.

5.2 Example: Wide-Field Observations

The wide-field HDRT will achieve an etendue ($A\Omega$) of between 150-600 m-degree^2

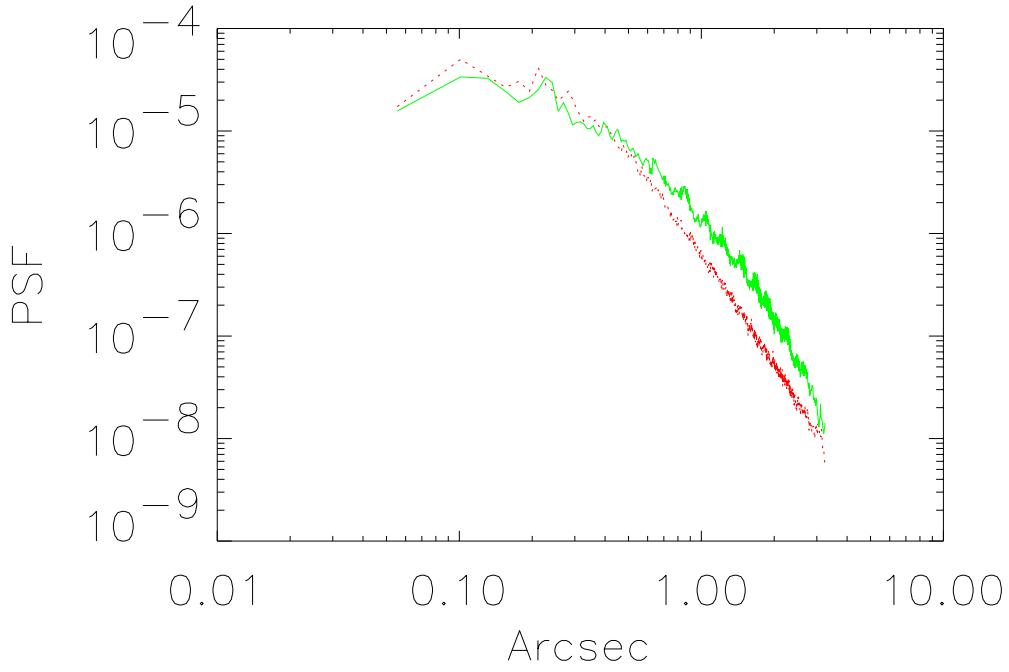

Figure 23: *The coronagraphic PSF from the HDRT (dotted/red) and KS (solid/green) telescopes.*

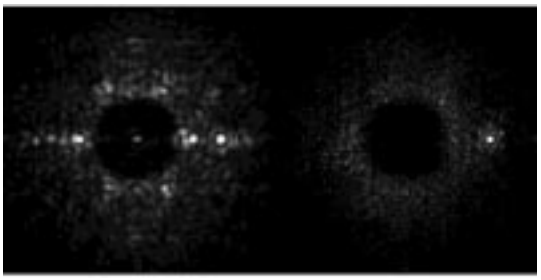

Figure 25: *Seeing averaged images from KS (left) and HDRT (right) telescopes after the Lyot coronagraph. The faint companion is unambiguously detected with the HDRT.*

(depending on whether we adopt the 1x1 or 2x2 deg^2 design) – more than an order of magnitude larger than existing telescopes and comparable to, or larger than, the $A\Omega$ product of the specialized single-function survey telescopes that are now under discussion. HDRT's non-refractive wide-field mode will allow deep visible and infrared surveys that sample the full-sky with broad-band and selective optical and IR sensitivity. A single broad-band 20 minute observation near a wavelength of 0.8μm reaches a sensitivity of about 30 magnitudes. A series of short, 15 sec observations could sample half of the sky with a 10-σ sensitivity of 25 mag in approximately 2-10 days. These capabilities will revolutionize studies of:

- Supernovae to high redshift,
- Weak gravitational lens tomography of the cosmic mass distribution,
- A complete statistical sample of KBO's, perhaps as large as 10,000 objects (100's of times larger than the current population),
- Faint optical and IR transients.
- All Near-earth objects larger than a few hundred meters.

6 ADAPTIVE OPTICS AND INSTRUMENTATION

A major concern for implementing AO on large-aperture telescopes is the very high dynamic range required from the wavefront correction system. The relative phase fluctuations due to the atmosphere between points separated a distance d grow as $(d/R_0)^{5/6}$ (Tatarski [6]). Thus, the actuator range required from a deformable mirror increases nearly linearly with the telescope aperture. For $R_0 = 1$ m turbulence a 15 m telescope must correct rms wavefront distortions corresponding to more than 3.6 waves. In a distributed pupil telescope like the HDRT it is straightforward to separately correct this large component of the turbulence (the average wavefront phase fluctuation between subapertures) with a physically distinct low order phase error correction scheme. One technique for doing this is described by Roddier [7].

The adaptive optics and active alignment systems of the HDRT are fundamental components of the telescope design. Its scientific impact depends on achieving diffraction limited performance over narrow fields, and seeing-limited capabilities over its wide-field. Certainly before this telescope is completed multi-conjugate and tomographic techniques will be devised to extend its useful diffraction limited field-of-view. For example, recently Fusco [8] estimated how the HDRT fov could be improved with three guide stars. With a 2 arcmin separation we may expect an fov of 2 to 3 arcmin. The larger, 22 m, parent mirror naturally improves the isoplanatic field-of-view over smaller aperture telescopes. Finally, it is notable that at wavelengths beyond about 8 μm the HDRT will often achieve its diffraction limit with only tip-tilt

correction.

The HDRT AO system, when considered as six 6.5m pupil systems, is no more complex than current large telescope AO systems. The UH/IfA curvature system on the Gemini telescope will shortly use an 85 actuator system, while the 400-element system we assumed for the calculations in this document uses only about 67 elements per mirror segment.

Our time-dependent AO simulations also show that the larger diameter HDRT mirrors lead to a decrease in the necessary temporal bandwidth of the AO control loop over a smaller segmented mirror telescope design. Relevant AO correction timescales depend on the size of the mirror divided by the velocity of the atmospheric phase screen overhead. The smaller mirror segments in the Keck-style format modulate speckle noise into the image plane at higher temporal frequencies than a design which uses larger distributed pupil subapertures.

The technology for maintaining the slow optical alignment of mirror segments at a level much less than a wavelength is now well demonstrated at Keck (*cf.* Chanan and Ohara [9]). We are confident that either active referenced mirror alignment techniques or indirect optical methods (cf. Roddier [7]) can be used to achieve the *active* pointing and piston alignment required for the HDRT mirror segments.

Given the enormous flexibility of the HDRT "optical bench" concept, a broad range of astronomical instruments will be used with it. Unfortunately, on any telescope the size of the HDRT it is difficult to consider routine instrument changes in the style of current CFHT operations. It seems likely that the next generation of telescopes will swap instruments only infrequently. Fortunately the HDRT unfilled pupil encourages a facility with permanently-mounted instrumentation. We envision a wide-field optical/IR imager and spectrograph along with coronagraphic visible and IR imagers and spectrographs for the narrow-field configuration. Each of these would be mounted to the telescope OSS, either near the back of the M1 mirror cell for WFM instruments or to the core of the telescope, near the top-end, for NFM instruments.

7 THE COST SCALE OF THE HDRT PROJECT

During the last century the worlds largest telescopes have evolved from the 1.5 m Yerkes refractor to the 10 m Keck (Fig. 26). It is interesting to notice that each of these projects advanced our state-of-the-art with a completely new set of telescope technologies. The transition from Yerkes to the Hooker marked the beginning of large reflectors, the Hooker to Hale telescopes involved fundamental changes in mirror and optical mount technologies, while the Keck telescope marked even greater changes in these technologies. With each new telescope the astronomical community succeeded in doubling the previous largest aperture diameter. As conceived, the HDRT will be a natural extrapolation of this evolution indicated in Fig. 26.

As a concept study, and given current HDRT design "freedoms", significant effort spent at this stage to estimate the cost of the HDRT would be wasted. Nevertheless it is important to understand which elements of the telescope design will determine most of the resource requirements and what the likely range of these budgets should be. "First-principle" estimates are not likely to be useful, so these figures are scaled from

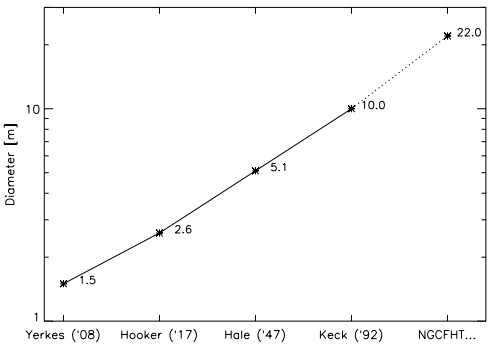

Figure 26: *The world's largest telescopes have evolved in a remarkably systematic fashion. The HDRT would extend this evolution.*

other telescope projects in consultation with local and REOSC engineering talent.

A useful estimate of the optics resource requirements comes from the VLT experience. In fact, the light gathering power of the four VLT telescopes is within a few percent of the HDRT. Based on the VLT we can estimate the total cost of the six HDRT M1 blanks to be about $ 18M with a comparable polishing cost. WFM-M3 may cost an additional $ 10M to acquire and polish, while WFM-M2 should require another $ 4M. The cost of NFM-M2 is less than $ 1M. The M1 active mirror cell(s) is likely to be about $ 10M. Assuming the telescope structure could be built for $ 15M, the enclosure for $ 15M, site work for $ 9M, software and controls at $ 10M, general design and management at $ 10M, and a contingency – we find that the cost scale of this project could be $ 150M.

Estimating the timescale for the HDRT is difficult but from other recent large telescope projects we expect that it will take about 8 years to polish the optics. A lower limit for the time to completion of HDRT is probably about ten years.

8 NEXT STEPS

The impetus for moving forward with large ground-based telescopes has been illustrated in documents like the U.S. "Decadal Review." Note that HDRT **will** satisfy many of the key science goals called out in that report. We believe that we must begin the hard process of finding scientific and financial partners for this enterprise now, while we have some momentum and greater potential of attracting the attention which is essential to secure a project of this magnitude. Thus our first priority would be to increase the public and community-wide awareness of the unique capabilities of the HDRT.

At the same time we must generate realistic cost and timeline projections. The key trade studies to be done include:

- A more detailed study of the aspherics and off-axis mirrors should be done to define the most efficient testing methods.
- Concept level multiconjugate AO solutions should be used to ensure that the final HDRT design takes full advantage of the wider diffraction limited fov.
- Telescope mount designs must be generated with sufficient detail to determine more realistic mass, resonance, and other mechanical system performance figures.
- Control systems for the optical and mechanical components need to be defined and modeled.
- Optical baffling design for the wide-field (and to a lesser degree the narrow-field mode) must be done to optimize visible and IR performance.

- An enclosure must be designed and evaluated against site requirements.
- Telescope operation and maintenance issues like mirror coating, safety, and other facility requirements must be evaluated.
- System level engineering requirements must be assessed.

While this task list is long and will indubitably grow, we feel it is important to move forward with design studies now if we are to benefit from the appoaching swell in enthusiasm for the next generation of ground-based telescopes. With this in mind we look forward to the next concept-level review of these design efforts within 18 months of this CFH21 meeting.

References

[1] Kuhn, J. R. and Hawley, S. L.: 1999, PASP 111, 601.

[2] Moretto, G. and J.R. Kuhn: 2000, App. Opt. 39, 2782.

[3] Moretto, G. and J.R. Kuhn: 1999, SPIE 3785, 73.

[4] Northcott, M.: 2000, personal communication.

[5] Lo, D.: 2000, Coast Steel, personal communication.

[6] Tatarski, V.I.: 1961 Wave Propagation in a Turbulent Medium (New York: McGraw-Hill).

[7] Roddier, F.: 2000, Dana Point Conf. "Working on the Fringe".

[8] Fusco, T.: 2000, "First MCAO Studies for the HDRT" (unpublished).

[9] Chanan, G. A., Ohara, C.M.: 2000, SPIE 4003, 188.